Table 3. Differentially Upregulated Genes in Liver of Chronic Hepatitis B

Gene	GenBank ID	*P* Value	*t* Value HBV/HCV*	Hep/Ly	GO: Molecular Function
Viral genome					
HBV-core	X01587	0.000	6.69	Hep	Viral genome
Cell cycle and growth related					
V-ets erythroblastosis virus E26 oncogene homolog 2	NM_005239	0.001	3.97	Hep/Ly	skeletal development
RAP2A, member of RAS oncogene family	AI698376	0.000	3.91	Hep/Ly	signal transduction
Melanoma antigen, family C, 1	NM_005462	0.001	3.76	Hep/Ly	regulation of transcription
Cell division cycle 27	NM_001256	0.001	3.54	Hep/Ly	cell proliferation
Cyclin H	NM_001239	0.000	3.10	Hep/Ly	DNA repair
Immune response					
Interferon regulatory factor 6	NM_006147	0.000	3.80	Hep	regulation of transcription, DNA-dependent
Proteoglycan 2, bone marrow	R28336	0.001	3.65	Hep/Ly	defense response to bacteria
Chemokine (C-C motif) ligand 16	AW827147	0.001	3.49	Hep/Ly	chemokine activity
Janus kinase 2 (a protein tyrosine kinase)	NM_004972	0.001	3.48	Ly	JAK-STAT cascade
Chemokine (C-X-C motif) receptor 3	NM_001504	0.000	3.03	Hep/Ly	G-protein coupled receptor protein signaling pathway
Cell death					
BCL2-associated athanogene 2	NM_004282	0.000	3.95	Hep	apoptosis
Fas (TNFRSF6) associated factor 1	AA831837	0.001	3.74	Hep/Ly	apoptosis
Proline dehydrogenase (oxidase) 1	R88591	0.000	3.73	Hep/Ly	induction of apoptosis by oxidative stress
Caspase 9, apoptosis-related cysteine protease	NM_032996	0.001	3.58	Hep/Ly	apoptotic program
Purinergic receptor P2X, ligand-gated ion channel, 1	NM_002558	0.003	3.52	Hep/Ly	apoptosis
Tumor suppressing subtransferable candidate 1	NM_003310	0.002	3.35	Hep/Ly	apoptosis
Tumor necrosis factor (ligand) superfamily, member 11	NM_033012	0.002	3.25	Hep	cell differentiation
Diablo homolog (*Drosophila*)	NM_019887	0.004	3.04	Hep	apoptosis
Cell communication					
Nexilin (F actin binding protein)	NM_144573	0.000	4.15	Hep/Ly	unknown
Neurogranin (protein kinase C substrate, RC3)	NM_006176	0.000	4.09	Hep	signal transduction
Collagen, type XV, alpha 1	NM_001855	0.000	4.08	Hep/Ly	extracellular matrix
Chromogranin B (secretogranin 1)	NM_001819	0.001	3.47	Hep/Ly	hormone activity
Prostaglandin I2 (prostacyclin) receptor (IP)	NM_000960	0.001	3.42	Ly	G-protein signaling
Integral membrane protein 2C	NM_030926	0.002	3.36	Ly	integral to membrane
Sperm autoantigenic protein 17	NM_017425	0.002	3.26	Hep/Ly	cAMP-dependent protein kinase regulator activity
Talin 2	AF007154		3.18	Ly	cell adhesion
Cadherin 16, KSP-cadherin	AI241319	0.003	3.11	Hep	cell adhesion
Syntaxin binding protein 6 (amisyn)	AA281449	0.004	3.03	Ly	cell adhesion
Stress response					
RAD51-like 1 (*S. cerevisiae*)	NM_002877	0.000	3.78	Hep/Ly	DNA repair
Metallothionein 1X†	BC053882	0.001	3.44	Hep	electron transport
Siah-interacting protein	AA069322	0.002	3.08	Hep/Ly	ubiquitin cycle
Metallothionein 2A‡	NM_005953	0.004	3.03	Hep	copper ion homeostasis
F-box and leucine-rich repeat protein 2	NM_012157	0.000	3.01	Hep/Ly	ubiquitin cycle
Development					
Wolf-Hirschhorn syndrome candidate 1	NM_133335	0.001	4.51	Hep/Ly	morphogenesis
Homeo box B2	AI292043	0.001	3.87	Hep/Ly	development
Neurogenic differentiation 1	NM_002500	0.000	3.38	Hep/Ly	cell differentiation
Opiate receptor-like 1	NM_000913	0.004	3.29	Hep/Ly	G-protein coupled receptor protein signaling pathway
Wingless-type MMTV integration site family, member 2B	NM_024494	0.002	3.14	Hep/Ly	frizzled-2 signaling pathway
Cell motility					
Oligophrenin 1	R81942	0.001	3.80	Hep/Ly	rho GTPase activator activity
ATP-binding cassette, subfamily C, member 9	H16193	0.004	3.06	Hep	transporters
Transporter					
Sodium channel, voltage gated, type VIII, alpha	NM_014191	0.004	3.78	Hep/Ly	cation transport
Enzymes					
HMT1 hnRNP methyltransferase-like 6 (*S. cerevisiae*)	NM_018137	0.001	4.44	Hep/Ly	s-adenosylmethionine-dependent methyltransferase
Chymotrypsin-like	NM_001907	0.001	3.74	Hep/Ly	negative regulation of blood coagula
Aspartoacylase (aminocyclase) 3§	NM_080658	0.005	3.26	Hep/Ly	metabolism
Transcription and signal transduction					
Hepatocyte nuclear factor 4, gamma	AW273065	0.000	4.38	Hep/Ly	regulation of transcription
Nuclear receptor coactivator 6	NM_014071	0.000	3.98	Hep/Ly	DNA recombination
Protein kinase C, gamma	NM_002739	0.001	3.88	Hep/Ly	intracellular signaling cascade
T-box 2	NM_005994	0.000	3.82	Hep/Ly	development
Zinc finger protein 167	NM_018651	0.003	3.49	Hep/Ly	regulation of transcription, DNA-dependent
Small nuclear ribonucleoprotein polypeptide A	AI491862	0.002	3.37	Hep/Ly	intracellular signaling cascade
Zinc finger protein 266	NM_198058	0.002	3.03	Ly	regulation of transcription, DNA-dependent

*The univariate *t*-statistics for comparing the classes are used as the weights. †3.9-fold induction, ‡7.7-fold induction, and §1.8-fold induction by IFN-α in Huh-7 cells

In accordance with pathway analysis, antigen-presenting major histocompatibility complex molecules and IFN-α-induced genes were preferentially upregulated in CH-C (Table 6, Fig. 3). Genes related to apoptosis, DNA repair and cell death were upregulated in CH-B. DNA repair and apoptosis-related transcription factors were upregulated in CH-B, whereas anti-apoptosis and cell proliferation-related transcription factors were upregulated in CH-C. Platelet activating factor was upregulated in CH-C. As for metabolism-related gene regulation, peroxisome-associated genes were

Table 4. Differentially Upregulated Genes in Liver of Chronic Hepatitis C

Gene	GenBank ID	*P* Value	*t* Value HCV/HBV	Hep/Ly	IFN Induced	GO: biological process
Cell cycle and growth related						
Hect domain and RLD 5	NM_016323	0.000	4.50	Hep/Ly	7.7	regulation of cyclin dependent protein kinase activity
Inhibitor of growth family, member 4	NM_198287	0.001	3.50	Hep/Ly		grow arest
Phosphoinositide-3-kinase, class 3	AI446184	0.001	3.42	Hep/Ly		inositol or phosphatidylinositol kinase activity
Non-metastatic cells 1, protein (NM23A) expressed in	NM_000269	0.002	3.28	Hep		CTP biosynthesis
Mitogen-activated protein kinase kinase kinase 10	AI991621	0.003	3.23	Hep/Ly		JNK cascade
Immune responces						
Interferon, alpha-inducible protein 27	NM_005532	0.000	6.29	Hep	2.4	response to pest, pathogen or paras
Interferon, alpha-inducible protein (clone IFI-15K)	NM_005101	0.000	4.65	Hep/Ly	27.9	cell-cell signaling
Myxovirus (influenza virus) resistance 1	NM_002462	0.000	4.28	Hep/Ly	49.9	
Cold autoinflammatory syndrome 1	NM_183395	0.000	4.14	Ly		inflammatory response
Interferon-stimulated transcription factor 3, gamma 48kD	NM_006084	0.000	3.89	Hep/Ly	1.8	immune response
Beta-2-microglobulin	NM_004048	0.001	3.63	Hep/Ly	2.7	antigen presentation, endogenous antigen
2'-5'-oligoadenylate synthetase 2 (69-71 kD)	AA731148	0.001	3.49	Hep/Ly	3.3	immune response
Interferon-induced protein 44-like	NM_006820	0.001	3.42	Ly	4.5	immune response
Apolipoprotein L, 3	AW002766	0.003	3.23	Ly		inflammatory response
Immunoglobulin kappa constant	BC062732	0.004	3.04	Ly		immune response
Cell death						
Defender against cell death 1	NM_001344	0.000	4.11	Hep/Ly		apoptosis
HIV-1 Tat interactive protein 2, 30kDa	NM_006410	0.004	3.03	Hep/Ly		induction of apoptosis
Cell communication						
Major histocompatibility complex, class I, C	NM_002117	0.001	3.74	Hep/Ly		antigen presentation
CD97 antigen	NM_078481	0.001	3.72	Ly		cell adhesion
Major histocompatibility complex, class I, B	NM_005514	0.002	3.38	Hep/Ly	1.9	antigen presentation
Carcinoembryonic antigen-related cell adhesion molecule 5	NM_004363	0.002	3.30	Hep/Ly		integral to plasma membrane
Major histocompatibility complex, class II, DQ beta 1	NM_002123	0.002	3.25	Ly		antigen presentation
Major histocompatibility complex, class II, DR beta 4	NM_022555	0.002	3.25	Hep/Ly		antigen presentation
Dystroglycan 1 (dystrophin-associated glycoprotein 1)	AI684076	0.003	3.14	Hep/Ly		extracellular matrix
Dipeptidylpeptidase 6	NM_130797	0.004	3.11	Hep/Ly		integral to membrane
Ubiquitin and proteasome system						
Proteasome (prosome, macropain) subunit, beta type, 8	U17496	0.000	4.55	Hep/Ly		immune response
Ubiquitin D	NM_006398	0.003	3.13	Ly	2.1	antimicrobial humoral response
Proteasome (prosome, macropain) 26S subunit, non-ATPase, 2	NM_002808	0.004	3.05	Hep/Ly		regulation of cell cycle
Translation						
Eukaryotic translation elongation factor 1 beta 2	AI262506	0.000	4.46	Ly		protein biosynthesis
Eukaryotic translation initiation factor 1A, Y-linked	NM_004681	0.003	3.19	Hep/Ly	5.3	protein biosynthesis
Lipid metabolism						
Diacylglycerol O-acyltransferase homolog 1 (mouse)	NM_012079	0.002	3.31	Hep/Ly		O-acyltransferase activity
24-dehydrocholesterol reductase	NM_014762	0.003	3.19	Hep		cholesterol biosynthesis
Carnitine palmitoyltransferase II	NM_000098	0.005	3.01	Hep/Ly		fatty acid beta-oxidation
Nucleotide metabolism						
Adenosine deaminase, RNA-specific	NM_015841	0.001	3.46	Hep/Ly		RNA editing
Topoisomerase (DNA) I	J03250	0.003	3.22	Hep/Ly		DNA unwinding
THO complex 1	L36529	0.003	3.15	Hep/Ly		nuclear mRNA splicing, via spliceosome
Karyopherin alpha 3 (importin alpha 4)	NM_002267	0.003	3.14	Hep/Ly		NLS-bearing substrate-nucleus import
Nicotinamide nucleotide adenylyltransferase 1	NM_022787	0.004	3.06	Hep/Ly		NAD biosynthesis
Nuclear autoantigenic sperm protein (histone-binding)	M97856	0.005	3.00	Hep/Ly		DNA packaging
Ribonucleotide reductase M2 polypeptide	NM_001034	0.005	3.00	Ly		DNA replication
G protein binding protein						
Regulator of G-protein signalling 10	NM_002925	0.002	3.38	Hep/Ly		signal transduction
Transcription and signal transduction						
Staphylococcal nuclease domain containing 1	NM_014390	0.000	4.60	Hep/Ly		development
Ring-box 1	NM_014248	0.001	3.61	Ly		protein ubiquitination
Trophinin	NM_177558	0.001	3.44	Ly		embryo implantation
Forkhead box F1	AI453333	0.001	3.18	Hep/Ly	2.5	regulation of transcription, DNA-dependent
Nuclear antigen Sp100	M60618	0.003	3.02	Hep/Ly	5.8	regulation of transcription, DNA-dependent
Zinc finger protein 211	NM_198855	0.004	3.02	Ly		regulation of transcription, DNA-dependent
GA binding protein transcription factor, beta subunit 2, 47kDa	NM_181427	0.004	3.02	Hep/Ly		regulation of transcription, DNA-dependent
LIM protein (similar to rat protein kinase C-binding enigma)	AI445592	0.004	3.01	Hep/Ly		heart development
Hematopoietic cell-specific Lyn substrate 1	NM_005335	0.005	3.00	Ly		intracellular signaling cascade
ADP-ribosylation factor 5	M57567	0.005	3.00	Hep/Ly		intracellular protein transport

upregulated in CH-B, whereas cholesterol biosynthesis was upregulated in CH-C.

To investigate these findings in more detail, lymphocytes and hepatocytes were separately isolated by LCM and their gene expression was examined (Table 6, Fig. 4A, Fig. 7). Cyclophilin A and cyclophilin C, encoding peptidyl-prolyl cis-trans isomerases, were upregulated in CH-C. A recent report describes inhibition of HCV replication in Huh-7 cells by cyclophilin.[23,24] The upregulation of ssDNA-binding genes, such as p53 and RAD, and the relative downregulation of mitochondrial genes in hepatocytes, in CH-B, reflect a strong DNA damage response inducing apoptosis. Many IFN-α-induced genes were upregulated in hepatocytes rather than lymphocytes in CH-C.

CD4, CD8, linker for activation of T cells, and pro-apoptotic genes were upregulated in lymphocytes

Table 5. Pathway Analysis

Frequent Pathway Process	P Value
Whole liver tissue in CHB (n = 19)	
Caspase activation via cytochrome c	7.04E-11
Regulation of transcription, DNA-dependent	1.66E-12
Intermediate filament-based process	1.24E-07
Calcium ion transport	9.08E-08
Regulation of blood pressure	2.94E-07
Protein amino acid phosphorylation	4.04E-07
Regulation of angiogenesis	5.35E-09
TGF-beta receptor signaling pathway	8.08E-11
Whole liver tissue in CHC (n = 20)	
Defense response	3.27E-06
Antigen presentation, endogenous antigen	6.79E-06
Golgi vesicle transport	5.22E-07
Lipid catabolism	6.61E-06
Regulation of cell cycle	2.43E-08
Regulation of cholesterol absorption	1.02E-05
EGF receptor signaling pathway	1.59E-09
Ubiquitin cycle	4.71E-05

in CH-B. Despite the activated T cell responses in CH-B, chemokine expression was induced more in the lymphocytes in CH-C than lymphocytes in CH-B (Fig. 4A). To examine the functional role of liver-infiltrating lymphocytes further, LCM samples were also obtained from 4 more patients with CH-B and 4 with CH-C. Gene expression was compared for lymphocyte subsets (84 CD markers, including 26 T cell makers, 21 B cell markers, 16 myeloid cell markers, 11 NK cell markers, and 12 AD markers). Among these, many T cell markers and Th1 cytokines were significantly more upregulated in CH-B than in CH-C lymphocytes. Conversely, B cell marker, Th2 cytokines, and chemokines were preferentially induced in CH-C (Fig. 4B-C). The differences in immune reaction in CH-B and CH-C may be a reflection of their different pathogenesis.

Detailed Gene Network Analysis of Differentially Expressed Genes in CH-B and CH-C. To obtain a detailed and comprehensive gene network underlying CH-B and CH-C, SAGE data were integrated with those from cDNA microarray analysis. We applied 361 upregulated genes in CH-B ($P < .05$) and 344 in CH-C ($P < .05$), obtained from cDNA microarray analysis, and 1924 upregulated genes in CH-B (more than 5-fold tag count differences) and 1780 in CH-C, obtained from SAGE analysis, to the construction of the knowledge-based gene network. To find the gene network among these induced genes, published results of interaction of individual genes were integrated with these results using MetaCore software. Direct interactions between individual genes were searched for. The gene network of these differentially expressed genes formed a complex interaction of individual genes; however, representative signaling pathways underlying CH-B or CH-C were identified (Fig. 5).

In CH-B, p53 and 14-3-3 interacting genes might play an important role in the induced signaling pathways. Transcriptional factors such as CCAAT/enhancer binding protein (C/EBP), c-JUN, and cAMP-responsive element binding protein 1 (CREB1) are possibly also important molecules regulating these signaling pathways. These molecules induced apoptosis and activated transcription and oncogenes. Such activation might activate

Table 6. Gene Ontology Comparison

GO Description	Number of Genes	LS Permutation (P Value)	KS Permutation (P Value)	HBV	HCV	Reference
Whole liver tissue						
Antigen presenting	15	0.00105	0.034	1.01	1.49	0.81
IFN-alpha induced	71	$<1 \times 10^{-5}$	0.000	1.49	2.09	1.16
Cell death	34	0.005	0.019	1.35	1.15	0.99
DNA repair	62	0.005	0.041	1.51	1.10	1.11
G_1/S transition of mitotic cell cycle	18	0.001	0.009	1.25	1.41	1.23
Transcription factor binding	74	0.017	0.001	1.33	1.33	1.30
Cholesterol biosynthesis	12	0.029	0.002	1.11	1.44	1.30
PDGF	22	0.005	0.012	1.08	1.33	1.13
Peroxisome	19	0.026	0.005	1.46	1.17	0.93
Hepatocytes						
Peptidyl-prolyl cis-trans isomerase activity	9	0.002	0.001	1.31	1.48	1.15
Single-stranded DNA binding	16	0.019	0.003	1.85	1.34	1.27
Mitochondria	110	0.005	0.010	0.89	1.52	1.14
IFN-alpha induced	77	0.004	0.146	1.62	5.77	1.35
Lymphocytes						
Immunological synapse	12	0.002	0.003	6.38	3.78	3.31
Induction of apoptosis via deathdomain receptors	7	0.004	0.018	1.53	1.02	1.07
Chemotaxis	54	0.004	0.069	1.35	1.78	1.14

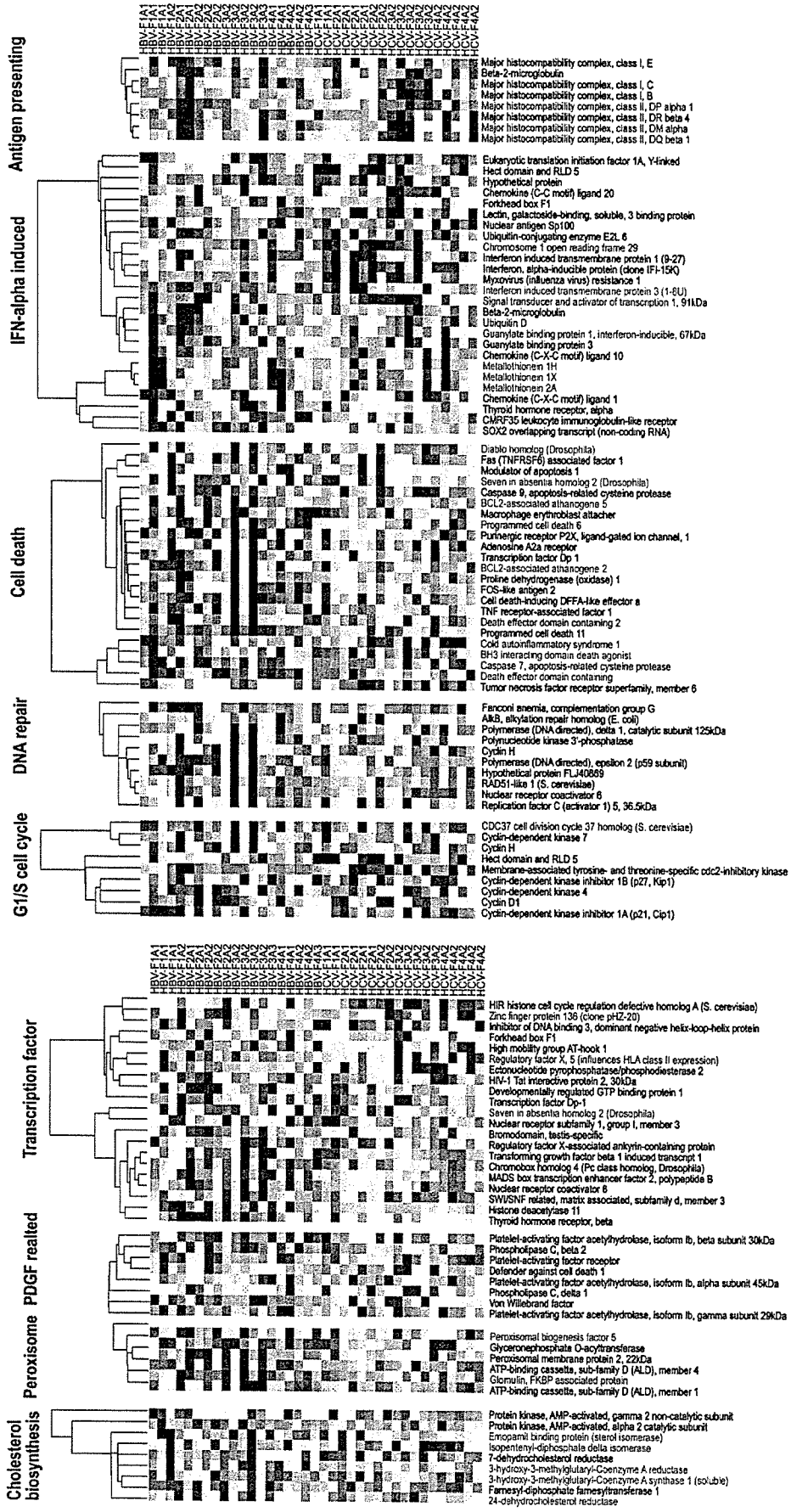

Fig. 3. One-way hierarchical clustering of whole liver samples with representative genes ($P < .05$) included in each GO category which was significantly different in CH-B and CH-C ($P < .005$). Green text denotes genes expressed predominantly in hepatocytes, and blue text denotes genes expressed predominantly in lymphocytes.

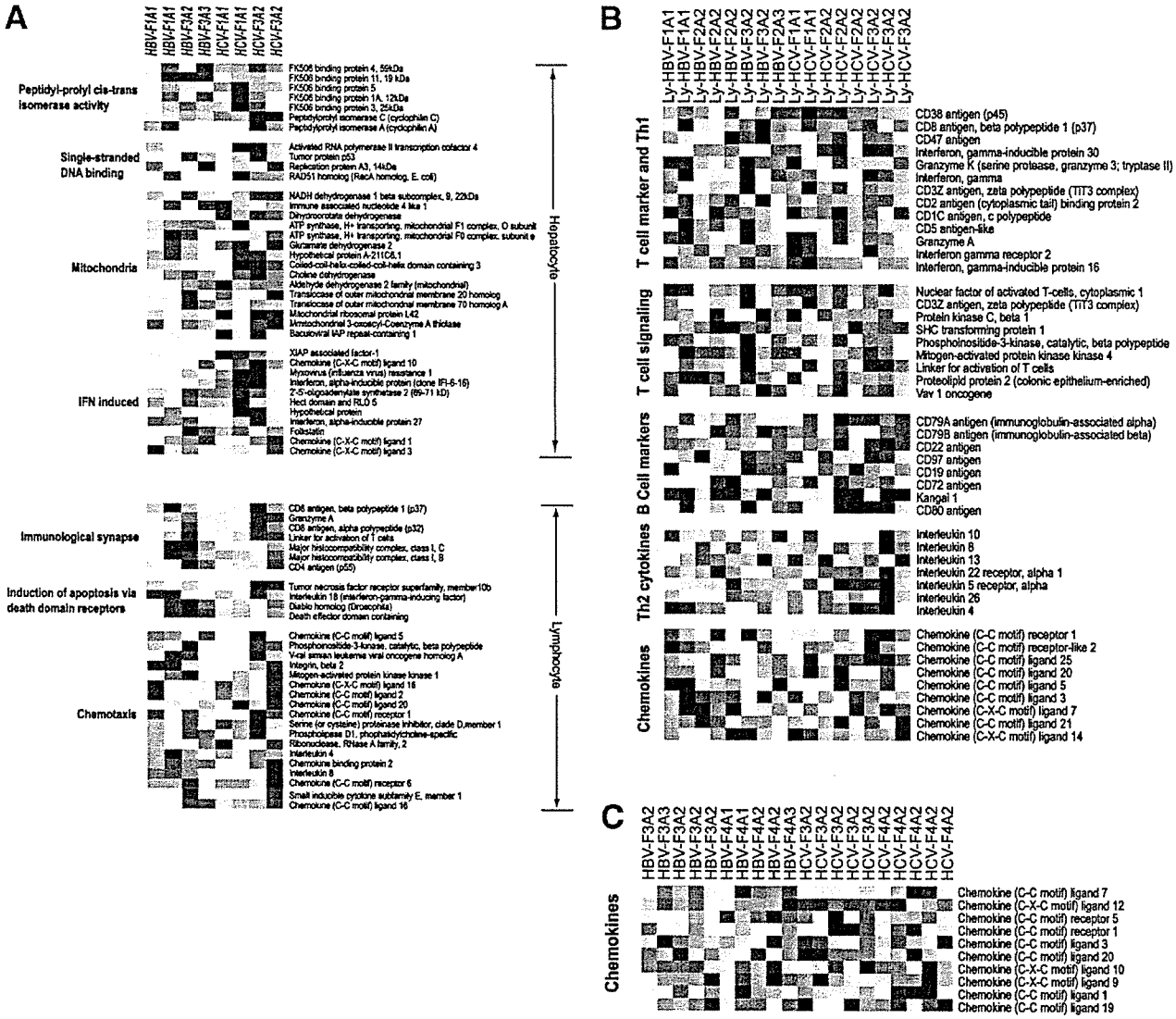

Fig. 4. (A) One-way hierarchical clustering of LCM samples with representative genes ($P < .05$). (B) One-way hierarchical clustering of liver-infiltrating lymphocytes, featuring specific gene sets of immune function. (c) One-way hierarchical clustering of whole liver sample gene sets of chemokines.

peroxisomes in CH-B (Fig. 5). In CH-C, type 1-IFN signaling (ISGF3/STAT1) might play a major role in the induced signaling pathways. The activation of the NF-κB and epidermal growth factor receptor (EGFR) signaling pathways may reflect liver inflammation and regeneration. These activations could lead to activation of liver X receptor/retinoid X receptor (LXR/RXR), a regulator of lipid metabolism.

Based on the database of MetaCore, which covers the entire regulation of the transcriptional factors, transcriptional regulation of differentially expressed genes was analyzed (Table 7). Transcription of mothers against decapentaplegic homolog 3 (SMAD 3), activator protein-1 (AP-1), p53, CREB1, and sterol regulatory element binding transcription factor 1 (SREB-1) was induced in CH-B, whereas NF-κB, IRF-1, STAT1, and retinoid acid receptor-alpha (RARα) signaling pathways were induced in CH-C. These differences fundamentally explain the different signaling pathways in CH-B and CH-C.

To examine whether these differences in gene expression contribute the different mechanism of hepatocarcinogenesis, we compared the angiogenic factors in CH-B and CH-C. The hierarchical clustering of patients using 34 angiogenesis-related genes obtained from cDNA microarray analysis, significantly clustered patients into 2 groups of CH-B or CH-C ($P = .0001$) (Fig. 6A). In CH-B, VEGF-family genes, FGF, and the angiopoietin

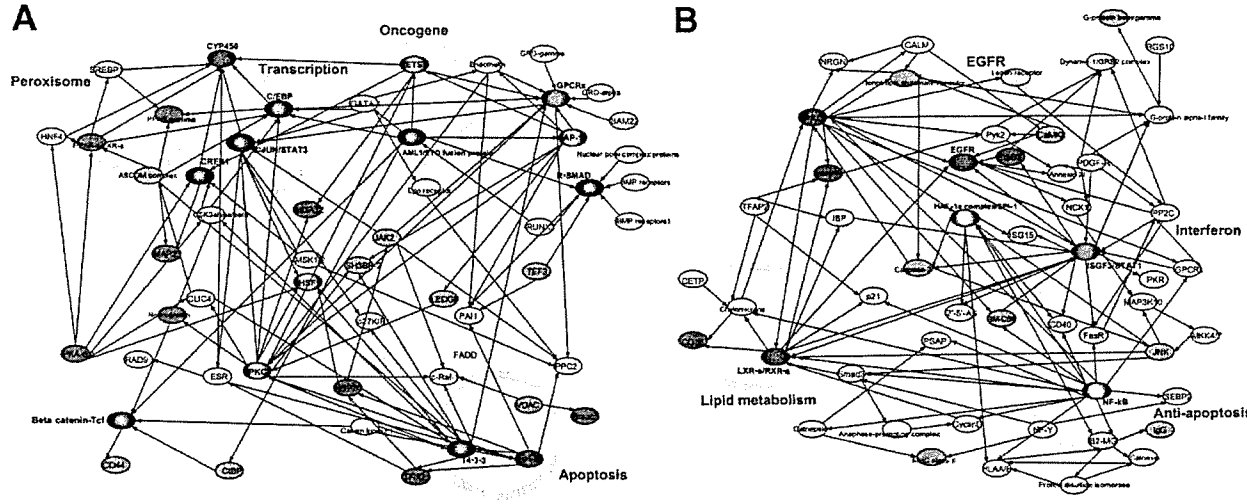

Fig. 5. (A) Gene network of differentially expressed genes in CH-B. (B) Gene network of differentially expressed genes in CH-C. Core transcription factors are represented by black ovals. Green ovals show genes expressed predominantly in hepatocytes and blue ovals show genes expressed predominantly in lymphocytes.

family were induced by several transcriptional factors including AP-1, c-fos, and STAT3, which were all strongly upregulated. In CH-C, inflammation-related angiogenic factors such as IL-8, IL-18, and PDGF1, induced by NF-κB, were also upregulated (Fig. 6B, Fig. 7). Thus, CH-B and CH-C showed different angiogenic properties, which implied that the tumorigenic process in CH-B and CH-C may differ.

Table 7. Transcription Regulation

	Frequent pathway process	*P* value
	Chronic hepatitis B	
1	Mothers against decapentaplegic homolog 3 (SMAD3)	5.25E-36
2	Activator protein-1 (AP-1)	4.24E-33
3	p53	8.49E-33
4	cAMP-responsive element binding protein 1 (CREB1)	2.39E-32
5	v-ets erythroblastosis virus E26 oncogene homolog 1 (ETS1)	3.38E-32
6	Sterol regulatory element binding transcription factor 1 (SREBP1)	6.73E-32
7	Transcription factor binding to IGHM enhancer 3 (TFE3)	9.48E-32
8	Signal transducer and activator of transcription 3 (STAT3)	1.33E-31
9	v-ets erythroblastosis virus E26 oncogene homolog 2 (ETS2)	1.88E-31
10	Transcription factor 7/Lymphoid enhancer binding factor 1 [Tcf(ref)]	1.88E-31
	Chronic hepatitis C	
1	Nuclear factor of κ light polypeptide gene enhancer in B-cells 1 (NF-κB)	1.32E-35
2	Interferon regulatory factor 1 (IRF1)	4.34E-33
3	Splicing factor 1(SF1)	9.17E-33
4	Signal transducer and activator of transcription 1 (STAT1)	1.28E-32
5	Retinoid acid receptor- (RAR)	1.81E-32
6	Nuclear factor of κ light polypeptide gene enhancer in B-cells 2 (RelA)	3.56E-32
7	Vitamin D receptor (VDR)	5.00E-32
8	Wilms tumor 1(WT1)	7.02E-32
9	Sterol regulatory element binding transcription factor 2 (SREBP2)	9.84E-32
10	Epidermal growth factor receptor (EGFR)	1.92E-31

Quantitative RTD-PCR. We performed quantitative real-time detection PCR (RTD-PCR) using 15 TaqMan probes. The results of RTD-PCR on whole liver biopsy and LCM samples are shown in Fig. 7. In CH-B, apoptosis-inducing genes such as CASP9, IFNG, GZMA, TP53, BGA2, and DIABLO were upregulated. In CH-C, IFN-α-induced genes and chemokines such as MxA, IFI15, OAS2, and IP10 were upregulated. Angiogenic factors such as FGFB, ANGPT1, and VEGF were upregulated in CH-B, and another angiogenic factor, PDECGF, was upregulated in CH-C. The results are consistent with those from the cDNA microarray.

Discussion

The biological activity of viral coding polyproteins of HBV and HCV has been extensively investigated in cell lines and in transgenic mouse models. For example, accumulated evidence shows HBV-X protein to be a transcriptional transactivator that interacts with p53 tumor suppressor protein, modulating its signaling pathway.[9,25] The transgenic mouse model with overexpression of HCV polyproteins in the liver develops steatosis and HCC.[26,27] However, these findings have not been well evaluated in clinical samples.

Using in-house cDNA microarray analysis of 1080 genes, we previously reported differing gene expression profiles of liver tissue from patients with CH-B and CH-C.[13] However, the detailed signaling pathways underlying these diseases needed further clarification. In this study,

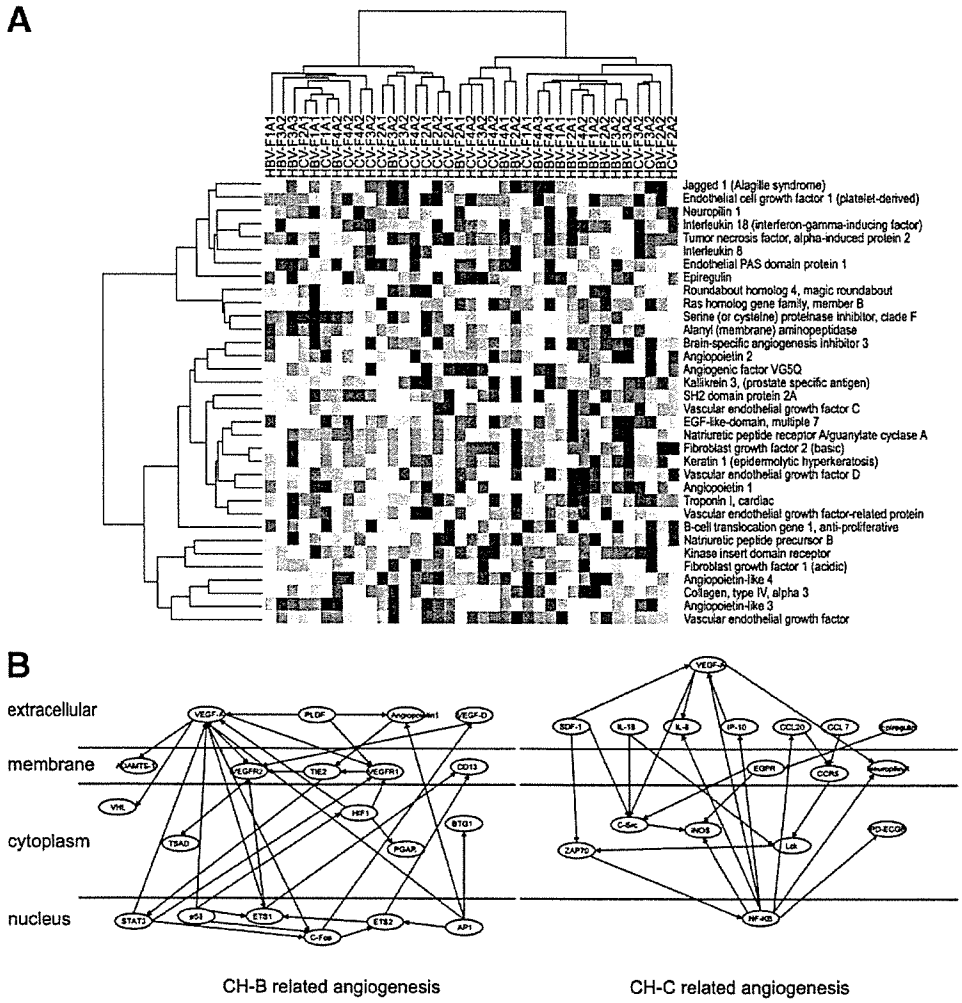

Fig. 6. (A) Hierarchical clustering of whole liver samples using angiogenic genes. (B) Gene network of angiogenic genes in CH-B and CH-C.

we constructed a new microarray slide, liver chip 10 K, consisting of 9614 clones which were selected from unique tag sequences in our hepatic SAGE libraries, including 667,067 tag sequences (manuscript in preparation), for the purpose of analyzing gene expression profiling in liver disease. We analyzed the gene expression profiles of whole liver biopsy specimens obtained from 37 patients with CH-B and CH-C. In addition, we selectively isolated liver-infiltrating lymphocytes (16 samples) and hepatocytes (8 samples) from liver biopsy specimens using LCM (Fig. 1D) and analyzed their gene expression. Furthermore, SAGE data were obtained from pooled samples of 3 CH-B or 3 CH-C patients, and their gene expression data were integrated to reveal the comprehensive, detailed gene network involved in CH-B and CH-C, respectively.

Hierarchical clustering analysis of 37 patients grouped these patients into 2 groups with CH-B or CH-C, with a few exceptions. Moreover, gene prediction analysis significantly discriminated between CH-B and CH-C patients ($P < .001$). HBV or HCV was the only factor significantly involved in patient classification, and other factors such as histological stage, disease activity, age, and ALT levels were not significantly associated with the classification of these patients. This indicates that virus type, whether HBV or HCV, influences liver gene expression to a greater degree than any other clinical parameter, such as degree of fibrosis or inflammation (Table 2).

The pathway analysis and GO comparison in CH-B and CH-C using whole liver biopsy revealed that antigen-presenting genes, IFN-α-induced genes, G_1/S transition genes, and cholesterol biosynthesis and platelet-derived factors were upregulated in CH-C, whereas genes related to cell death, DNA repair, and peroxisomes were upregulated in CH-B (Tables 5-6, Fig. 3). The association of HCV infection with steatosis in the liver in CH-C has

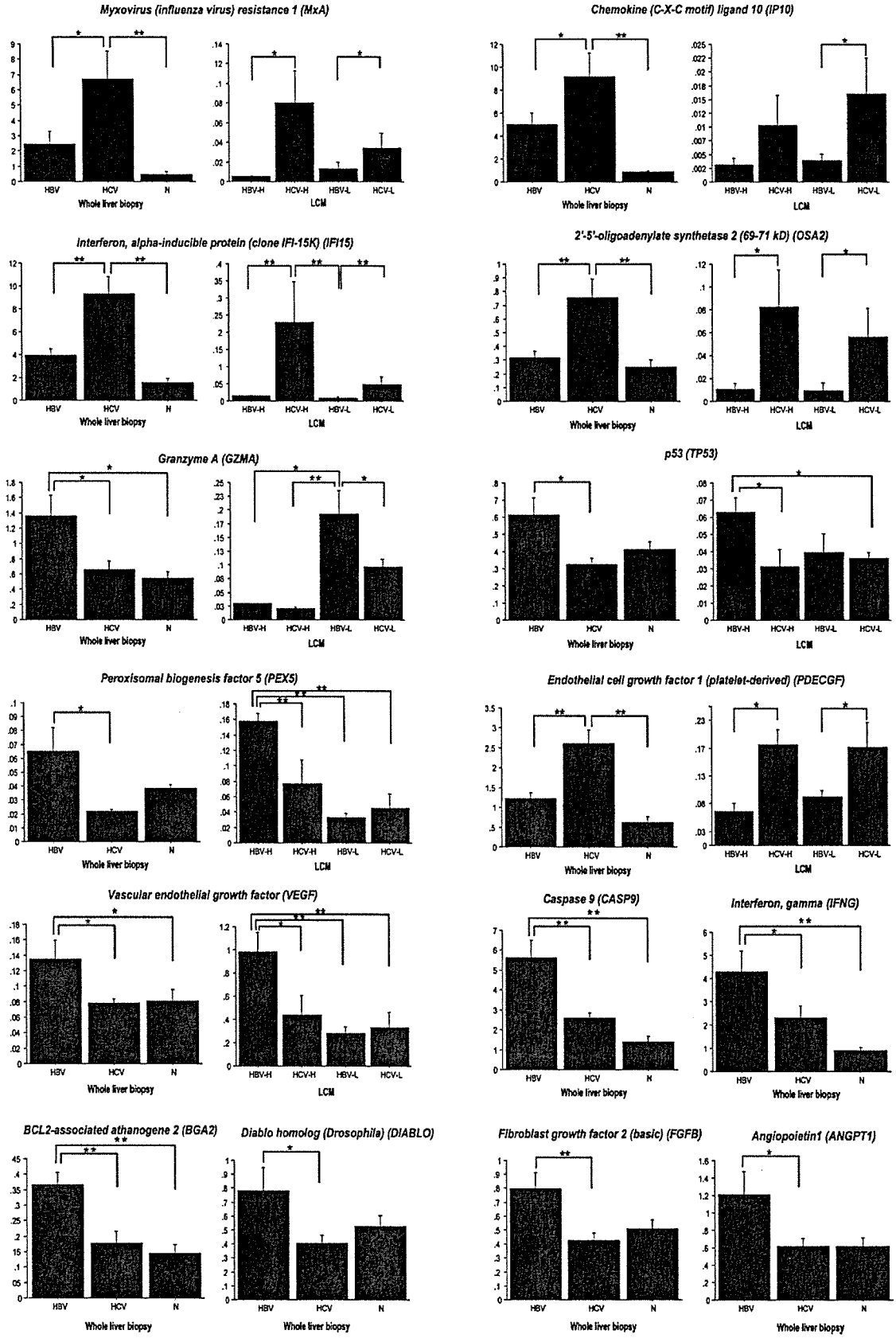

Fig. 7. Quantitative real-time detection PCR (RTD-PCR) using 15 TaqMan probes. The results of whole liver biopsy (HBV; 19 samples of CH-B, HCV; 18 samples of CH-C and N; 6 samples of normal liver) and LCM samples (HBV-H; 4 samples of hepatocyte in CH-B, HCV-H; 4 samples of hepatocyte in CH-C, HBV-Ly; 8 samples of lymphocyte in CH-B, HCV-Ly; 8 samples of lymphocyte in CH-C) were shown. $*P < .05$, $**P < .01$.

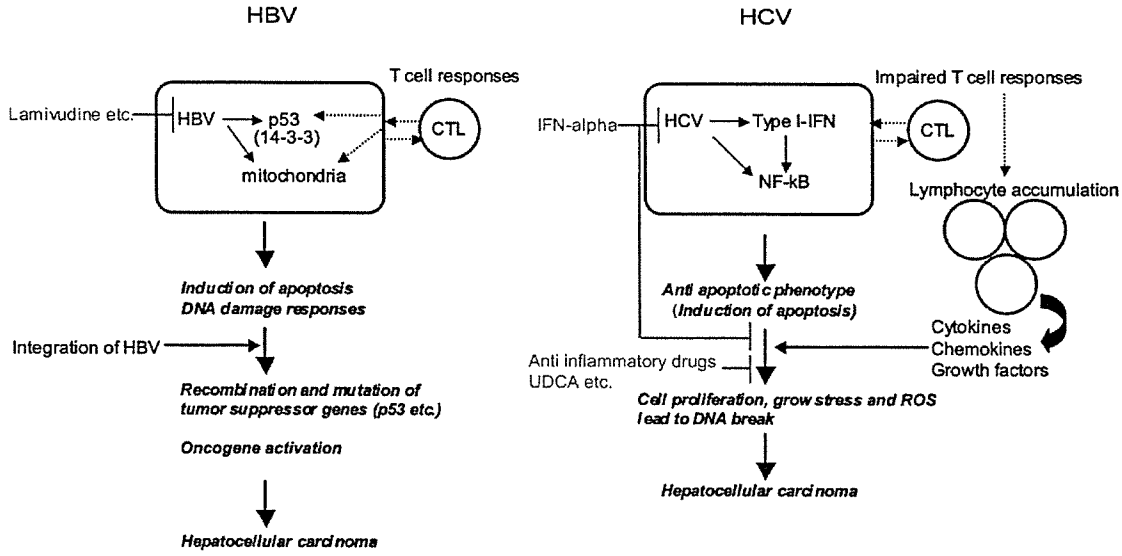

Fig. 8. Schematic representation of different pathogenesis of hepatitis and development of HCC in CH-B and CH-C.

been reported.[28,29] There might also be an association between HBV replication and peroxisomal activation, as reported using hepatoma-derived cell lines.[30,31] We combined SAGE data with those from cDNA microarray analysis and constructed the detailed and comprehensive gene network underlying CH-B and CH-C. In CH-B, p53-mediated and 14-3-3-mediated pro-apoptotic signaling; transcription factors such as AP-1, C/EBP, c-JUN, and CREB1; and oncogenes and peroxisomes were activated (Fig. 5). In CH-C, type 1-IFN (ISGF3/STAT1), NF-κB, EGFR, and LXR/RXR signaling were activated.

Lesion-specific gene expression analysis by LCM revealed more precise differences in gene expression between CH-B and CH-C (Fig. 4, Fig. 7), although a larger number of samples will be needed to reach concrete conclusions. Interestingly, many IFN-α-induced genes were upregulated in hepatocytes, but not in lymphocytes, in CH-C. On the other hand, DNA repair genes such as p53 and RAD were induced in hepatocytes in CH-B. Detailed analysis of lymphocyte markers revealed Th1-dominant responses in the liver in CH-B and Th2-dominant responses in the liver in CH-C.

Despite greater lymphocyte infiltration and homing in the liver, a weak T cell response and no T cell accumulation were observed in CH-C.[32,33] These contributed to the induction of various chemokines, cytokines, and growth factors, which may lead to cell proliferation and angiogenesis in CH-C. Surprisingly, gene expression profiling of angiogenic factors revealed clear differences in CH-B and CH-C. Many of the chemokines involved in angiogenesis are independent of VEGF-mediated or angiopoietin-mediated signaling pathways.[34] These findings possibly reflect a different means of carcinogenesis of HCC in CH-B and CH-C (Fig. 6).

In summary, we investigated the detailed signaling pathways in CH-B and CH-C. Although our data reveal the different signaling pathways induced in CH-B and CH-C, the precise mechanisms underlining these differences must be proven experimentally in the future. Nevertheless, from the therapeutic point of view, these results might be indicative that antiviral agents will be most effective for CH-B whereas anti-inflammatory drugs, other than IFN, would be effective for CH-C, for the prevention of HCC (Fig. 8). Further studies are needed to elucidate these findings clinically and biologically.

Acknowledgment: We thank Masami Ueda and Mikiko Nakamura for excellent technical assistance.

References

1. Shafritz DA, Shouval D, Sherman HI, Hadziyannis SJ, Kew MC. Integration of hepatitis B virus DNA into the genome of liver cells in chronic liver disease and hepatocellular carcinoma. Studies in percutaneous liver biopsies and post-mortem tissue specimens. N Engl J Med 1981;305:1067-1073.
2. Choo QL, Kuo G, Weiner AJ, Overby LR, Bradley DW, Houghton M. Isolation of a cDNA clone derived from a blood-borne non-A, non-B viral hepatitis genome. Science 1989;244:359-362.
3. Kiyosawa K, Sodeyama T, Tanaka E, Gibo Y, Yoshizawa K, Nakano Y, et al. Interrelationship of blood transfusion, non-A, non-B hepatitis and hepatocellular carcinoma: analysis by detection of antibody to hepatitis C virus. HEPATOLOGY 1990;12:671-675.
4. Huang HP, Tsuei DJ, Wang KJ, Chen YL, Ni YH, Jeng YM, et al. Differential integration rates of hepatitis B virus DNA in the liver of children with chronic hepatitis B virus infection and hepatocellular carcinoma. J Gastroenterol Hepatol 2005;20:1206-1214.

5. Minami M, Daimon Y, Mori K, Takashima H, Nakajima T, Itoh Y, et al. Hepatitis B virus-related insertional mutagenesis in chronic hepatitis B patients as an early drastic genetic change leading to hepatocarcinogenesis. Oncogene 2005;24:4340-4348.
6. Kim CM, Koike K, Saito I, Miyamura T, Jay G. HBx gene of hepatitis B virus induces liver cancer in transgenic mice. Nature 1991;351:317-320.
7. Murakami S, Cheong JH, Kaneko S. Human hepatitis virus X gene encodes a regulatory domain that represses transactivation of X protein. J Biol Chem 1994;269:15118-15123.
8. Murakami S, Cheong J, Ohno S, Matsushima K, Kaneko S. Transactivation of human hepatitis B virus X protein, HBx, operates through a mechanism distinct from protein kinase C and okadaic acid activation pathways. Virology 1994;199:243-246.
9. Lin Y, Nomura T, Yamashita T, Dorjsuren D, Tang H, Murakami S. The transactivation and p53-interacting functions of hepatitis B virus X protein are mutually interfering but distinct. Cancer Res 1997;57:5137-5142.
10. Yasui K, Wakita T, Tsukiyama-Kohara K, Funahashi SI, Ichikawa M, Kajita T, et al. The native form and maturation process of hepatitis C virus core protein. J Virol 1998;72:6048-6055.
11. Hsieh TY, Matsumoto M, Chou HC, Schneider R, Hwang SB, Lee AS, et al. Hepatitis C virus core protein interacts with heterogeneous nuclear ribonucleoprotein K. J Biol Chem 1998;273:17651-17659.
12. Colombari R, Dhillon AP, Piazzola E, Tomezzoli AA, Angelini GP, Capra F, et al. Chronic hepatitis in multiple virus infection: histopathological evaluation. Histopathology 1993;22:319-325.
13. Honda M, Kaneko S, Kawai H, Shirota Y, Kobayashi K. Differential gene expression between chronic hepatitis B and C hepatic lesion. Gastroenterology 2001;120:955-966.
14. Desmet VJ, Gerber M, Hoofnagle JH, Manns M, Scheuer PJ. Classification of chronic hepatitis: diagnosis, grading and staging. HEPATOLOGY 1994;19:1513-1520.
15. Shirota Y, Kaneko S, Honda M, Kawai HF, Kobayashi K. Identification of differentially expressed genes in hepatocellular carcinoma with cDNA microarrays. HEPATOLOGY 2001;33:832-840.
16. Kawai HF, Kaneko S, Honda M, Shirota Y, Kobayashi K. Alpha-fetoprotein-producing hepatoma cell lines share common expression profiles of genes in various categories demonstrated by cDNA microarray analysis. HEPATOLOGY 2001;33:676-691.
17. Kawaguchi K, Honda M, Yamashita T, Shirota Y, Kaneko S. Differential gene alteration among hepatoma cell lines demonstrated by cDNA microarray-based comparative genomic hybridization. Biochem Biophys Res Commun 2005;329:370-380.
18. Honda M, Kawai H, Shirota Y, Yamashita T, Kaneko S. Differential gene expression profiles in stage I primary biliary cirrhosis. Am J Gastroenterol 2005;100:2019-2030.
19. Honda M, Kawai H, Shirota Y, Yamashita T, Takamura T, Kaneko S. cDNA microarray analysis of autoimmune hepatitis, primary biliary cirrhosis and consecutive disease manifestation. J Autoimmun 2005;25:133-140.
20. Yamashita T, Hashimoto S, Kaneko S, Nagai S, Toyoda N, Suzuki T, et al. Comprehensive gene expression profile of a normal human liver. Biochem Biophys Res Commun 2000;269:110-116.
21. Yamashita T, Kaneko S, Hashimoto S, Sato T, Nagai S, Toyoda N, et al. Serial analysis of gene expression in chronic hepatitis C and hepatocellular carcinoma. Biochem Biophys Res Commun 2001;282:647-654.
22. Mootha VK, Lindgren CM, Eriksson KF, Subramanian A, Sihag S, Lehar J, et al. PGC-1alpha-responsive genes involved in oxidative phosphorylation are coordinately downregulated in human diabetes. Nat Genet 2003; 34:267-273.
23. Watashi K, Ishii N, Hijikata M, Inoue D, Murata T, Miyanari Y, et al. Cyclophilin B is a functional regulator of hepatitis C virus RNA polymerase. Mol Cell 2005;19:111-122.
24. Nakagawa M, Sakamoto N, Tanabe Y, Koyama T, Itsui Y, Takeda Y, et al. Suppression of hepatitis C virus replication by cyclosporin a is mediated by blockade of cyclophilins. Gastroenterology 2005;129:1031-1041.
25. Lin Y, Nomura T, Cheong J, Dorjsuren D, Iida K, Murakami S. Hepatitis B virus X protein is a transcriptional modulator that communicates with transcription factor IIB and the RNA polymerase II subunit 5. J Biol Chem 1997;272:7132-7139.
26. Moriya K, Fujie H, Shintani Y, Yotsuyanagi H, Tsutsumi T, Ishibashi K, et al. The core protein of hepatitis C virus induces hepatocellular carcinoma in transgenic mice. Nat Med 1998;4:1065-1067.
27. Lerat H, Honda M, Beard MR, Loesch K, Sun J, Yang Y, et al. Steatosis and liver cancer in transgenic mice expressing the structural and nonstructural proteins of hepatitis C virus. Gastroenterology 2002;122:352-365.
28. Adinolfi LE, Gambardella M, Andreana A, Tripodi MF, Utili R, Ruggiero G. Steatosis accelerates the progression of liver damage of chronic hepatitis C patients and correlates with specific HCV genotype and visceral obesity. HEPATOLOGY 2001;33:1358-1364.
29. Monto A, Alonzo J, Watson JJ, Grunfeld C, Wright TL. Steatosis in chronic hepatitis C: relative contributions of obesity, diabetes mellitus, and alcohol. HEPATOLOGY 2002;36:729-736.
30. Raney AK, Kline EF, Tang H, McLachlan A. Transcription and replication of a natural hepatitis B virus nucleocapsid promoter variant is regulated in vivo by peroxisome proliferators. Virology 2001;289:239-251.
31. Guidotti LG, Eggers CM, Raney AK, Chi SY, Peters JM, Gonzalez FJ, et al. In vivo regulation of hepatitis B virus replication by peroxisome proliferators. J Virol 1999;73:10377-10386.
32. Murakami J, Shimizu Y, Kashii Y, Kato T, Minemura M, Okada K, et al. Functional B-cell response in intrahepatic lymphoid follicles in chronic hepatitis C. HEPATOLOGY 1999;30:143-150.
33. Racanelli V, Sansonno D, Piccoli C, D'Amore FP, Tucci FA, Dammacco F. Molecular characterization of B cell clonal expansions in the liver of chronically hepatitis C virus-infected patients. J Immunol 2001;167:21-29.
34. Guleng B, Tateishi K, Ohta M, Kanai F, Jazag A, Ijichi H, et al. Blockade of the stromal cell-derived factor-1/CXCR4 axis attenuates in vivo tumor growth by inhibiting angiogenesis in a vascular endothelial growth factor-independent manner. Cancer Res 2005;65:5864-5871.

MAJOR ARTICLE

Expression Profiling of Peripheral-Blood Mononuclear Cells from Patients with Chronic Hepatitis C Undergoing Interferon Therapy

Makoto Tateno,[1] Masao Honda,[1] Takashi Kawamura,[2] Hiroyuki Honda,[2] and Shuichi Kaneko[1]

[1]Department of Cancer Gene Regulation, Kanazawa University Graduate School of Medical Science, Kanazawa, and [2]Department of Biotechnology, School of Engineering, Nagoya University, Nagoya, Japan

q1 ***Background.*** Interferon (IFN) is now the standard treatment for chronic hepatitis C (CH-C); however, treatment efficacy is unpredictable before IFN therapy is started.

Methods. We investigated the gene-expression profiles of peripheral-blood mononuclear cells (PBMCs) from patients with CH-C showing different responses to IFN. Gene-expression profiles of PBMCs were analyzed in 21 q2 patients with CH-C treated with IFN alone or in combination with ribavirin as well as in 6 healthy volunteers. Serial changes in the gene-expression profiles of PBMCs from individual patients were evaluated before treatment, 2 weeks after the start of IFN therapy, and 6 months after the completion of IFN therapy.

Results. Interestingly, the gene-expression profiles of PBMCs from patients with CH-C and healthy volunteers differed substantially; early T cell–activation antigen CD69 was significantly up-regulated in patients with CH-C, but immune-related molecules such as chemokine (C-C motif) receptor 2 and interleukin 7 receptor were significantly down-regulated. Selected combinations of expressed genes obtained before treatment and during IFN q3 therapy by use of a fuzzy neural network combined with the SWEEP operator method predicted the outcome of IFN therapy with peak accuracies of 91.0% and 90.2%, respectively.

Conclusions. These findings suggest that the gene-expression profiles of PBMCs from patients with CH-C may q4 be useful biomarkers for IFN therapy.

Although interferon (IFN) is currently the standard treatment for patients with chronic hepatitis C (CH-C), only 30%–40% of patients completely eliminate the virus, even after effective IFN and ribavirin combination therapy [1–3]. The mechanism of viral persistence during IFN treatment remains to be clarified. It has been reported that several clinical factors, such as viral load, genotype, degree of fibrosis, and expression of type I IFN receptors, are useful predictive factors for the outcome of IFN therapy [4–6]; however, precise prediction is not possible at present.

q5 Type I IFN, such as IFN-α and IFN-β, plays an important role in innate immunity against viral infections by suppressing viral replication [7, 8]. However, the biological activities of IFN have not been fully elucidated. In viral infections such as measles, the number of peripheral lymphocytes generally decreases. It has also been reported that infection of dendritic cells and other immunocompetent cells is involved in exacerbated disease states and persistent infection [9]. Hence, it may be possible to assess disease state and severity by examining peripheral-blood mononuclear cells (PBMCs) from infected individuals. PBMCs include lymphocytes and monocytes, which play the most important roles in the immunological response to viral infection.

In the present study, we investigated the gene-expression profiles of PBMCs from patients with CH-C and healthy volunteers by use of cDNA microarray techniques [10–16]. By determining the gene-expression profiles of PBMCs from patients with CH-C receiving IFN therapy, we also clarified the differences in the PBMC gene-expression profiles between patients

Received 30 May 2006; accepted 23 August 2006; electronically published XX December 2006.

Potential conflicts of interest: none reported.

Reprints or correspondence: Shuichi Kaneko, Dept. of Cancer Gene Regulation, Kanazawa University Graduate School of Medical Science, 13-1, Takara-Machi, Kanazawa 920-8641, Japan (skaneko@medf.m.kanazawa-u.ac.jp).

The Journal of Infectious Diseases 2007;195:000–000

0022-1899/2007/19502-00XX$15.00

Table 1. Clinical characteristics of patients and responses to interferon (IFN) therapy.

Group, patient (sex, age in years)	ALT level, IU/L	Histology score	Serotype	IFN therapy	Response	Serum HCV RNA level, kIU/mL			PBMC HCV RNA at 2 weeks
						Before	2 weeks	6 months	
Group A									
1 (M, 46)	31	F1/A1	2	Mono	CR	23	<0.5	<0.5	–
2 (F, 47)	40	F1/A1	2	Mono	CR	416	<0.5	<0.5	+
3 (M, 71)	59	F4/A2	1	Mono	CR	42.3	2.2	<0.5	–
4 (M, 55)	19	F4/A2	2	Mono	CR	1.3	<0.5	<0.5	–
5 (M, 54)	30	F2/A1	1	Mono	BR	620	ND	>850	ND
6 (F, 43)	46	F2/A1	1	Mono	BR	160	<0.5	611	+
7 (M, 58)	236	F1-2/A1	NA	Mono	BR	360	<0.5	620	–
8 (M, 60)	114	F3/A2	2	Mono	BR	770	<0.5	2200	–
9 (M, 62)	70	F2/A1	1	Mono	NR	130	130	350	+
10 (M, 42)	59	F2/A1	1	Mono	NR	800	7.2	190	–
11 (F, 62)	138	F2-3/A2	2	Mono	NR	650	183	1400	+
12 (M, 49)	48	F2/A2	2	Mono	NR	330	<0.5	69.5	–
13 (F, 56)	104	F1/A1	1	Mono	NR	751	<0.5	610	–
Group B									
14 (M, 49)	69	F3/A2	1	Combination	CR	>850	ND	<0.5	ND
15 (M, 50)	35	F1/A2	1	Combination	CR	475	<0.5	<0.5	ND
16 (M, 44)	106	F2/A2	1	Combination	NR	325	68.8	82.6	ND
17 (M, 56)	30	F2/A1	1	Combination	CR	91	<0.5	<0.5	ND
18 (F, 39)	47	F1/A1	1	Combination	CR	>850	0.7	<0.5	ND
19 (F, 64)	117	F2/A1	1	Combination	NR	484	0.8	>850	ND
20 (M, 66)	31	F2/A1	1	Combination	NR	>850	390	1300	ND
21 (F, 62)	103	F3/A2	1	Combination	NR	820	270	1200	ND

NOTE. +, positive; –, negative; ALT; alanine aminotransferase; BR, biological responder; CR, complete responder; F, female; M, male; NA; not applicable ND; not detected; NR, nonresponder; PBMC, peripheral-blood mononuclear cell.

with CH-C who responded to IFN therapy (complete responders [CRs]) and those who did not (nonresponders [NRs]).

SUBJECTS, MATERIALS, AND METHODS

Patients. Subjects were 21 patients with CH-C and 7 patients who showed no clinical signs of hepatitis at Kanazawa University Hospital, Japan, between 1999 and 2001. To 13 patients with CH-C (group A), 6 million IUs of IFN-α2b was administered every day for 2 weeks and then 3 times weekly for 22 weeks. To 8 patients with CH-C (group B), IFN-α2b was administered in the same fashion, and ribavirin was administered concomitantly (600 mg for ≤60 kg of body weight, 800 mg for 60–80 kg of body weight, and 1000 mg for >80 kg of body weight). The 6 age- and sex-matched healthy volunteers were seronegative for either hepatitis B surface antigen or hepatitis C virus (HCV) antibody and had liver function values within normal limits. Eight CRs (negative HCV RNA for >6 months), 4 biochemical responders (BRs; normal serum alanine aminotransferase [ALT] levels for >6 months and positive serum HCV RNA), and 9 NRs to IFN therapy were enrolled. After informed consent was obtained from patients, peripheral-blood samples were collected before the start of IFN therapy, at 2 weeks into treatment, and at 6 months after the completion of treatment. PBMCs were then isolated from whole blood and stored in liquid nitrogen until use. Grading and staging of chronic hepatitis were histologically assessed according to the method of Desmet et al. [17]. Clinical characteristics, such as sex, age, ALT levels, degree of histological activity or staging, HCV RNA load and HCV serotype, did not differ significantly among the groups (table 1).

Virological assessment. The amount of HCV RNA was assayed by the Amplicor Monitor Test (Roche Molecular Systems). HCV was classified by a serologic genotyping assay that has been shown to be specific and sensitive for determining HCV genome subtype [18].

Preparation of cDNA microarray slides. Most cDNA clones used in the present study were obtained from IMAGE Consortium libraries through their distributor, Research Genetics, as described elsewhere [19–24]. In addition to these clones, we included clones to monitor IFN signaling. The newly constructed cDNA microarray slide (Kanazawa IFN chip; version 1.0) comprised 400 representative IFN signaling–related genes, 200 receptor- and cell adhesion–related genes, 160 apoptosis- and cell cycle–related genes, 150 transcription factors, 120 stress-response genes, and 275 other functional genes.

RNA isolation and antisense RNA amplification. Total

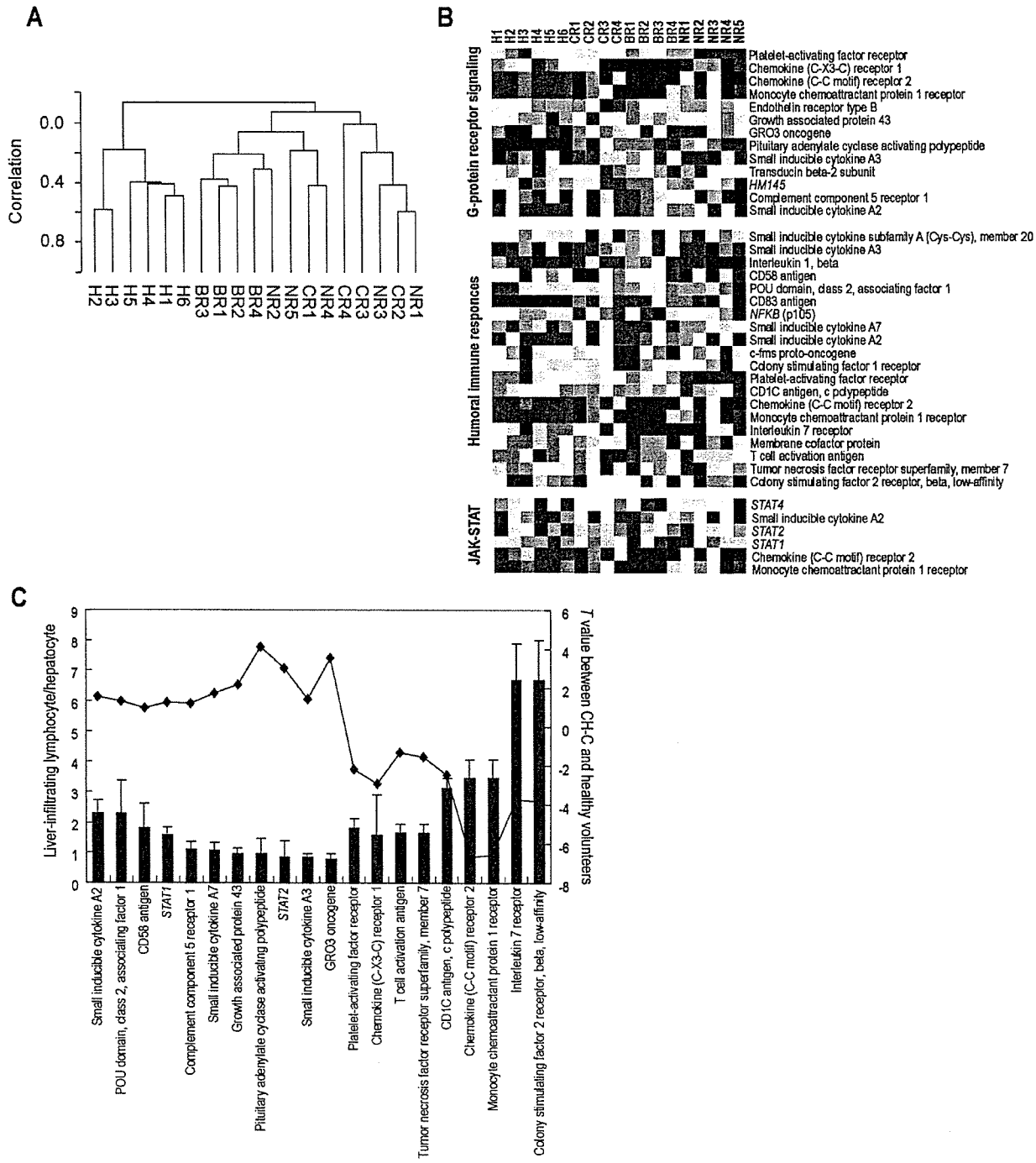

Figure 1. *A,* Hierarchical clustering analysis of gene-expression profiles of peripheral-blood mononuclear cell (PBMC) samples from 13 patients with chronic hepatitis C (CH-C; complete responders [CRs] 1–4, biochemical responders [BRs] 1–4, and nonresponders [NRs] 1–5) and 6 healthy volunteers (H1–H6) among 1305 tested genes before the start of interferon (IFN) therapy, performed using BRB-ArrayTools software. The dendrogram indicates the order in which patients were grouped on the basis of similarities in their gene-expression patterns. *B,* One-way clustering analysis of gene-expression profiles of PBMCs before the start of IFN therapy, using differentially expressed genes in the Janus kinase signal transducer and activation of transcription cascade, humoral immune response, and G protein–coupled receptor protein signaling pathway. Gene cluster data are presented graphically as colored images, red indicates up-regulated genes, and blue indicates down-regulated genes. *C,* Bar graph indicating gene expression in liver-infiltrating lymphocytes relative to that in hepatocytes *(left axis)* and line graph indicating the *T* values for class-prediction analysis between patients with CH-C and healthy volunteers *(right axis).* Genes with increased expression in the liver *(red)* tended to be expressed at lower levels in PBMCs, and genes with decreased expression in the liver *(blue)* tended to be expressed at higher levels in PBMCs.

Table 2. Representative up- or down-regulated genes in patients with chronic hepatitis C, compared with that in healthy volunteers.

Category, gene name	Ratio	*T*	*P*	GenBank accession no.	Gene annotation
Up-regulated					
CD83 antigen (activated B lymphocytes, immunoglobulin superfamily)	3.60	4.26	.00125	NM_004233	Defense response
Thrombospondin 1	3.29	5.19	.00014	NM_003246	Endopeptidase inhibitor activity
CD69 antigen (p60, early T cell–activation antigen)	2.87	5.55	.00001	NM_001781	Transmembrane receptor activity
Regulator of G protein signaling 1	2.33	4.31	.00029	NM_002922	Signal transducer activity
Pituitary adenylate cyclase–activating polypeptide	2.01	4.12	.00046	NM_001117	Neuropeptide hormone activity
Nicotinamide N-methyltransferase	1.99	5.29	.00003	NM_006169	Methyltransferase activity
Clone rasi-1 matrix metalloproteinase RASI-1	1.70	4.56	.00019	NM_002429	Hydrolase activity
VASP, exons 4–13	1.68	4.35	.00026	NM_003370	Actin binding
Xeroderma pigmentosum, complementation group A	1.63	3.86	.00085	NM_000380	Damaged DNA binding
Urokinase-type plasminogen activator receptor; GPI-anchored form precursor *(UPAR);* monocyte-activation antigen Mo3; CD87 antigen	1.53	4.41	.00023	NM_002659	Protein binding
Down-regulated					
Chemokine (C-C motif) receptor 2	0.35	−6.69	.00000	NM_000647	C-C chemokine receptor activity
Interleukin 7 receptor	0.47	−3.69	.00129	NM_002185	Antigen binding
Annexin II (lipocortin II)	0.49	−4.86	.00007	NM_004039	Calcium ion binding
Colony stimulating factor 2 receptor β, low-affinity (granulocyte-macrophage)	0.52	−3.85	.00088	NM_000395	Interleukin 3 receptor activity
Cytoplasmic dynein light chain	0.53	−4.12	.00046	NM_003746	Enzyme inhibitor activity
Ribosomal protein L13a	0.55	−3.94	.00070	X56932	Structural constituent of ribosome
Ikaros/LyF-1 homolog	0.56	−4.30	.00029	NM_006060	DNA binding
Chaperonin-containing TCP1, subunit 4 (Δ)	0.56	−4.60	.00014	NM_006430	Unfolded protein binding
Eosinophil Charcot-Leyden crystal (CLC) protein (lysophospholipase)	0.57	−3.73	.00116	NM_001828	Hydrolase activity
Myeloid cell nuclear differentiation antigen	0.57	−3.66	.00138	M81750	DNA binding
Ribosomal protein S16	0.59	−3.84	.00091	M60854	Structural constituent of ribosome
FK506-binding protein 4 (59 kD)	0.62	−4.28	.00030	NM_002014	Isomerase activity
Transforming growth factor β receptor IIB	0.62	−3.87	.00082	NM_003242	Type II transforming growth factor β receptor activity
Ribosomal protein L3	0.62	−3.80	.00099	X73460	Structural constituent of ribosome
KIAA0053	0.63	−5.73	.00001	D29642.1	GTPase activator activity
Peptidylprolyl isomerase D (cyclophilin D)	0.65	−4.71	.00011	NM_005038	FK506 binding
Citrate synthase	0.66	−5.54	.00001	NM_004077	Transferase activity
FADD	0.66	−3.72	.00119	NM_003824	Protein binding
C-myc oncogene	0.66	−3.84	.00089	NM_002467	Transcription factor activity
Interferon regulatory factor 2	0.66	−3.60	.00159	NM_002199	RNA polymerase II transcription factor activity
Intercellular adhesion molecule 3	0.66	−4.30	.00029	NM_002162	Protein binding

Table 3. Gene ontology (GO) comparison to discriminate between patients with chronic hepatitis C and healthy volunteers.

GO category	GO description	Genes, no.	*P* LS permutation	*P* KS permutation
7259	JAK-STAT cascade	6	.00167	.17913
6959	Humoral immune response	25	.00303	.03114
7186	G protein–coupled receptor protein signaling pathway	18	.00348	.17617

NOTE. JAK-STAT, Janus kinase signal transducer and activation of transcription.

RNA from PBMCs was isolated using Micro RNA Isolation Kits (Stratagene), and antisense RNA (aRNA) was amplified as described elsewhere [20, 22, 24]. The quality and degradation of isolated RNA were estimated after electrophoresis using an Agilent 2001 bioanalyzer. The references used for each microarray analysis were aRNA samples prepared from PBMCs obtained from a volunteer. Microarray hybridization was performed as described elsewhere [19–24], and each hybridization was repeated for all samples.

Gene-expression profiles of liver-infiltrating lymphocytes in patients with CH-C were investigated by laser-capture microdissection (LCM). Infiltrated lymphoid cells in the portal area and hepatocytes in liver-biopsy specimens obtained from 8 patients with CH-C were isolated by LCM. After 2 rounds of total

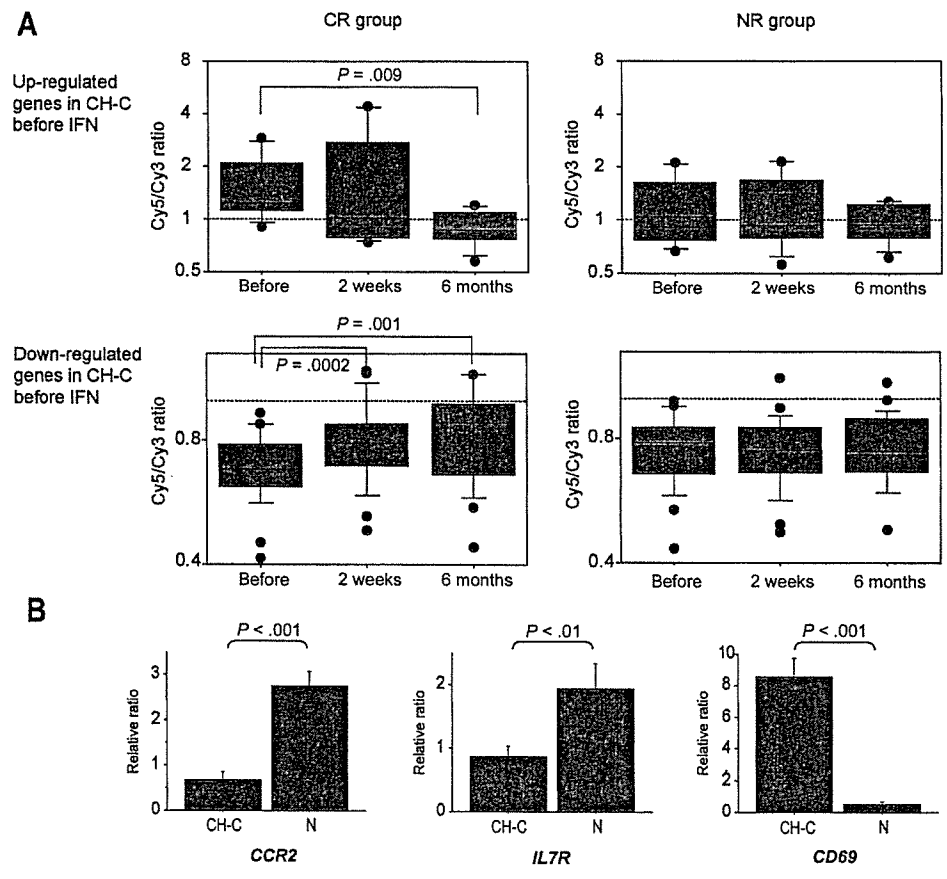

Figure 2. *A*, Changes in gene-expression profiles over the course of interferon (IFN) therapy (as shown in table 2) distinguishing patients with chronic hepatitis C (CH-C) from healthy volunteers before the start of IFN therapy. Box charts show average rates of change in relation to healthy volunteers as index functions. *B*, Real-Time polymerase chain reaction data for *CCR2* and *IL7R*, which were down-regulated (as determined on the basis of microarray data) in patients with CH-C before the start of IFN therapy, and *CD69*, which was up-regulated in patients with CH-C.

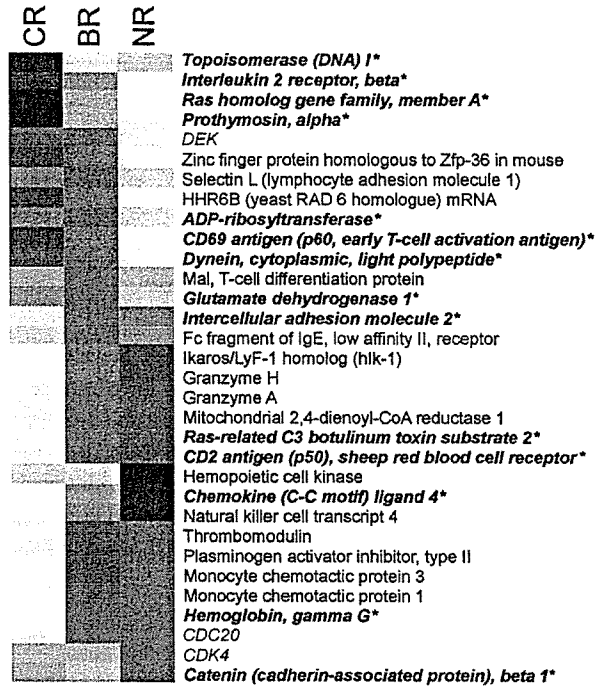

Figure 3. Thirty-two genes screened for gene-expression data before interferon (IFN) therapy by projective adaptive resonance theory. Red indicates up-regulated genes, and blue indicates down-regulated genes. Asterisks indicate genes that present similar expression patterns during IFN and ribavirin combination therapy. BR, biochemical responder; CR, complete responder; NR, nonresponder.

RNA amplification, the gene expression in infiltrated lymphoid cells was compared with that in hepatocytes [25]. Optimal conditions for LCM and reproducibility of data were assessed repeatedly [24, 25]. Some of these data were used for the analysis of genes expression.

Image analysis and data processing. Quantitative assessment of signals on the slides was performed using a ScanArray 5000 device (General Scanning), followed by image analysis q11 using QuantArray software (General Scanning).

Hierarchical clustering of gene expression in patients was performed using BRB-ArrayTools software (available at: http:/ q12 /linus.nci.nih.gov/BRB-ArrayTools.html). Filtered data were log transferred, normalized, centered, and applied to the average linkage clustering with centered correlation. BRB-ArrayTools include class comparison and class prediction tools based on univariate F tests to identify genes differentially expressed between predefined clinical groups. The permutation distribution of the F statistic, based on 2000 random permutations, was also used to confirm statistical significance. $P < .05$, as well as >1.5-fold differences in gene expression, were considered to be significant. A gene ontology (GO) comparison tool provides a list that has more genes differentially expressed and is coordinately regulated among predefined clinical groups than expected by chance and enables findings among biologically related genes to reinforce one another. Fisher and Kolmogorov-Smirnov tests were performed for GO comparison ($P < .005$) (BRB-ArrayTools).

Changes in gene expression in patients receiving IFN therapy were classified on the basis of self-organizing maps (GeneCluster software; version 2.0; available at: http://www.broad.mit.edu/cancer/software/genecluster2/gc2.html).

To identify class predictor genes for IFN therapy, projective adaptive resonance theory (PART) was used as a screening method for cDNA microarray data; unlike conventional clustering methods, PART enables the elimination of nonspecific dimensions for clustering from high-dimensional data [28–30]. From the genes extracted by PART, class predictor genes were selected using a fuzzy neural network (FNN) combined with the SWEEP operator method (FNN-SWEEP method). An FNN model with 1 input unit was initially created. Expression data for genes from data sets for patients with CH-C were entered into the FNN model, and the weight parameter was determined by the SWEEP operator method. We repeated this procedure for all genes to construct a model for each gene. The 10 genes with the highest accuracy levels were selected as the "first gene." The parameter increasing method was then applied. Having the first gene fixed, we used a similar method to select the second gene, which gave the highest accuracy in combination with the

Table 4. Ten gene combinations selected by the SWEEP operator method for construction of chronic hepatitis C class prediction at the start of interferon (IFN) therapy.

Combination	Input	Gene name	GenBank accession no.	Accuracy, %	
				Training	Test
1	1	***CD2 antigen (p50), sheep red blood cell receptor***[a]	NM_001767	21.2	14.1
	2	Glutamate dehydrogenase 1	NM_005271	72.4	46.2
	3	Dynein, cytoplasmic, light polypeptide	NM_003746	55.8	49.4
2	1	Ras-related C3 botulinum toxin substrate 2	NM_002872	34.6	20.5
	2	Glutamate dehydrogenase 1	NM_005271	81.4	68.6
	3	***Interleukin 2 receptor β***[a]	NM_000878	53.2	43.6
3	1	***Hemoglobin γG***[a]	NM_000184	19.9	16.7
	2	Ras-related C3 botulinum toxin substrate 2	NM_002872	64.7	36.6
	3	Dynein, cytoplasmic, light polypeptide	NM_003746	62.2	58.3
4	1	Intercellular adhesion molecule 2	NM_000873	28.9	26.3
	2	Ras homolog gene family member A	NM_001664	41.7	25.7
	3	Prothymosin α	NM_002823	66.0	47.4
5	1	Topoisomerase (DNA) I	NM_003286	53.9	46.2
	2	Catenin (cadherin-associated protein) β1 (88 kD)	NM_001904	66.0	57.1
	3	Ras-related C3 botulinum toxin substrate 2	NM_002872	91.0	89.1
6	1	Catenin (cadherin-associated protein) β1 (88 kD)	NM_001904	44.9	41.0
	2	Topoisomerase (DNA) I	NM_003286	66.0	57.1
	3	Ras-related C3 botulinum toxin substrate 2	NM_002872	91.0	89.1
7	1	Catenin (cadherin-associated protein) β1 (88 kD)	NM_001904	35.3	31.4
	2	***Interleukin 2 receptor β***[a]	NM_000878	47.4	43.6
	3	ADP-ribosyltransferase (NAD+; poly [ADP-ribose] polymerase)	NM_001618	62.2	60.9
8	1	Chemokine (C-C motif) ligand 4	NM_002984	44.9	41.0
	2	***Interleukin 2 receptor β***[a]	NM_000878	37.8	29.5
	3	Topoisomerase (DNA) I	NM_003286	44.9	34.6
9	1	***Interleukin 2 receptor β***[a]	NM_000878	30.8	30.8
	2	Catenin (cadherin-associated protein) β1 (88 kD)	NM_001904	47.4	43.6
	3	ADP-ribosyltransferase (NAD+; poly [ADP-ribose] polymerase)	NM_001618	62.2	60.9
10	1	CD69 antigen (p60, early T cell–activation antigen)	NM_001781	42.3	32.1
	2	Prothymosin α	NM_002823	33.3	24.4
	3	Glutamate dehydrogenase 1	NM_005271	39.1	31.4

[a] Genes that present similar expression patterns during IFN and ribavirin combination therapy.

first gene. Having the first gene and the second gene fixed, we selected the third gene. For validation of this model, we performed leave-one-out cross-validation (LOOCV); we left out 1 test sample and used the remaining 12 samples as training samples. We created 13 such sets. The FNN model was built up for 12 test samples, and the accuracy of training and test samples was calculated.

Real-time quantitative reverse-transcription polymerase chain reaction (RT-PCR). Quantitation of chemokine (C-C motif) receptor 2 *(CCR2), CD69,* and interleukin 7 receptor *(IL7R)* RNA expression was performed using the TaqMan real-rime PCR assay (ABI PRISM 7700 Sequence Detection System; PE Applied Biosystems), as described elsewhere [22, 23].

Statistical analysis. All data are expressed as mean ± SE values. One-way analysis of variance by the Bonferroni method or Student's *t* test was used to determine the significance of differences in clinical characteristics between patients in this study. $P < .05$ was considered to be significant.

RESULTS

cDNA microarray analysis of expression profiles of PBMCs from patients with CH-C. We initially compared the PBMC gene-expression profiles of patients with CH-C with those of healthy volunteers. For all 1305 genes, the results of hierarchical clustering analysis, a nonsupervised learning method, confirmed that the gene-expression profiles of PBMCs from the 6 healthy volunteers clearly differed when compared with those of the 13 patients with CH-C (group A) before IFN therapy (figure 1*A*). When the 2 groups were compared by support

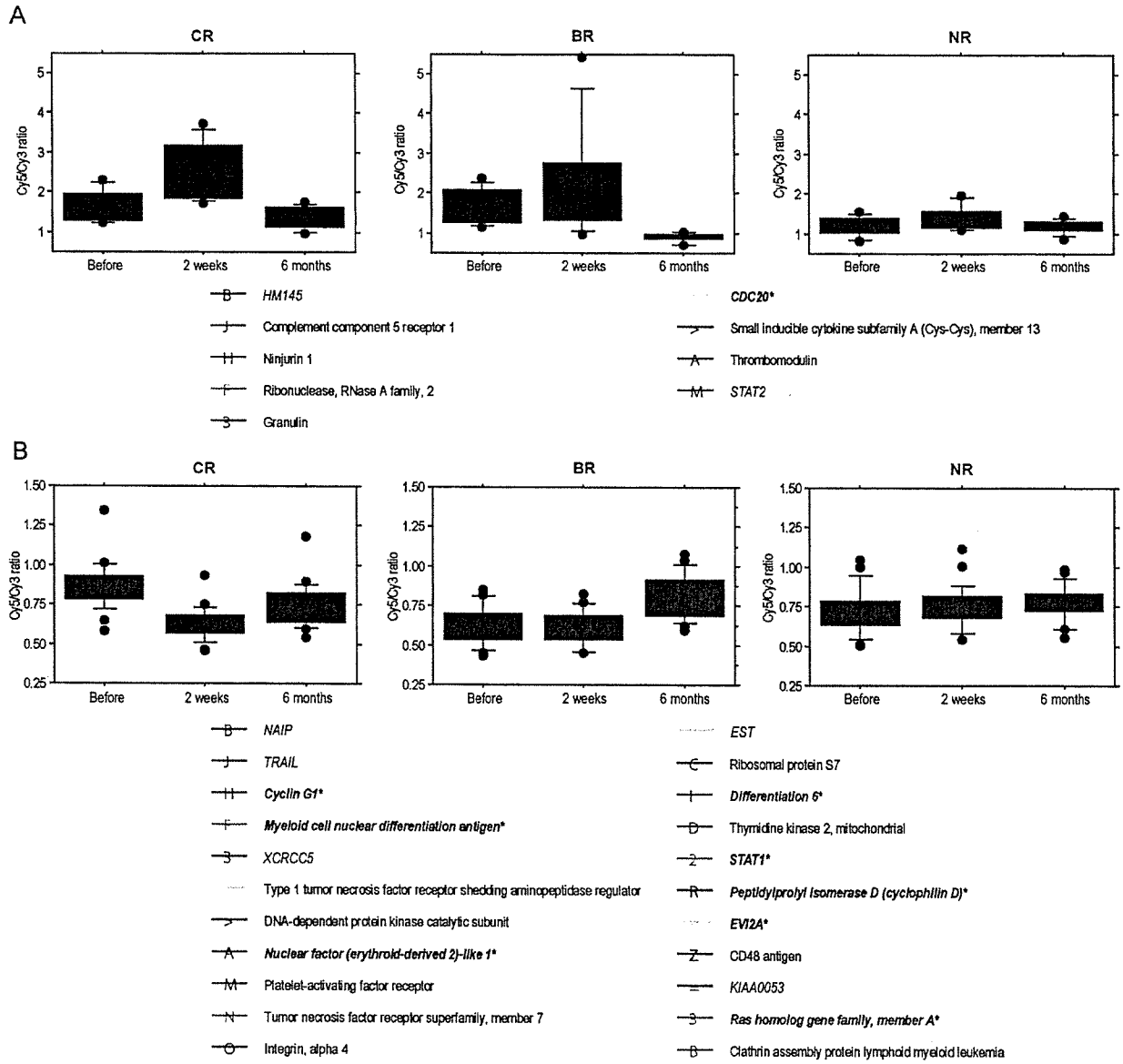

Figure 4. Gene-expression patterns. By use of projective adaptive resonance theory, 86 genes with changes in gene expression before and 2 weeks after the start of interferon (IFN) therapy were selected. For the complete responder (CR) group, changes in the expression of the 86 genes due to IFN therapy were classified into the following 5 patterns, on the basis of self-organizing maps (GeneCluster): up-regulated at 2 weeks after the start of IFN therapy and then down-regulated after the end of IFN therapy *(A);* down-regulated at 2 weeks after the start of IFN therapy and then up-regulated after the end of IFN therapy *(B);* up-regulated at 2 weeks after the start of IFN therapy and also up-regulated after the end of IFN therapy *(C);* up-regulated at 2 weeks after the start of IFN therapy and then returned to normal after the end of IFN therapy *(D);* and down-regulated at 2 weeks after the start of IFN therapy and also down-regulated after the end of IFN therapy *(E).* Representative genes are listed under each pattern. Asterisks indicate genes that present similar expression patterns during IFN and ribavirin combination therapy.

vector machine, a supervised learning method (BRB-ArrayTools), a total of 48 predictor genes were identified with a significance level of $P < .002$, and it was possible to differentiate the 2 groups with 100% accuracy. Gene parameters (ratio, *T* value, *P* value, description, GenBank accession no., and annotation) are summarized in table 2. q13

A GO comparison tool (BRB-ArrayTools) identifies more genes that are differentially expressed and are coordinately reg-

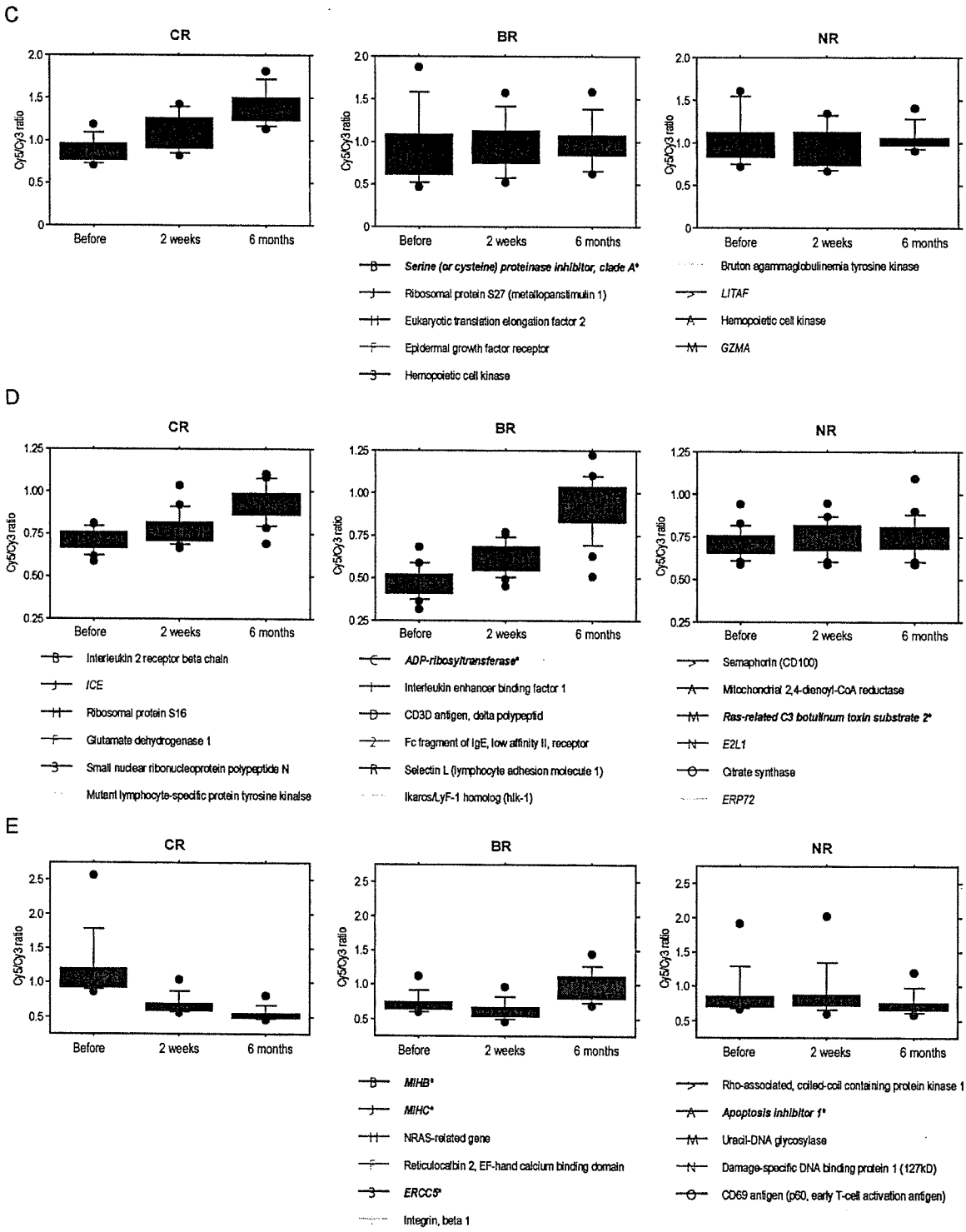

Figure 4. *(Continued.)*

Table 5. Ten gene combinations selected by the SWEEP operator method for the construction of chronic hepatitis C class prediction 2 weeks after the start of interferon (IFN) therapy.

Combination	Input	Gene name	GenBank accession no.	Accuracy, %	
				Training	Test
1	1	*ERCC5*	NM_000123	55.3	45.5
	2	Serine (or cysteine) proteinase inhibitor clade A member 1	NM_000295	85.6	54.5
	3	Ras homolog gene family member A	NM_001664	80.3	70.5
2	1	Baculoviral IAP repeat–containing 2	NM_001166	47.7	41.7
	2	Serine (or cysteine) proteinase inhibitor clade A member 1	NM_000295	80.3	53.8
	3	Ras homolog gene family member A	NM_001664	80.3	70.5
3	1	Cyclin G1	NM_004060	36.6	44.0
	2	Ras-related C3 botulinum toxin substrate 2	NM_002872	79.6	61.4
	3	*EST*		70.5	56.8
4	1	Ecotropic viral integration site 2A	NM_001003927	41.7	25.8
	2	Peptidylprolyl isomerase D (cyclophilin D)	NM_005038	60.6	46.2
	3	Cyclin G1	NM_004060	77.3	67.4
5	1	***Myeloid cell nuclear differentiation antigen***[a]	NM_002432	55.3	25.8
	2	Cyclin G1	NM_004060	85.6	64.4
	3	ADP-ribosyltransferase (NAD+; poly [ADP-ribose] polymerase)	NM_001618	80.3	87.1
6	1	Integrin β1	NM_033666	47.7	19.7
	2	Cyclin G1	NM_004060	80.3	62.9
	3	***STAT1AB***[a]	NM_139266	80.3	68.2
7	1	Differentiation 6 (septin 2)	NM_004404	28.8	25.8
	2	Cyclin G1	NM_004060	75.0	64.4
	3	Cell division cycle 20 homolog *(S. cerevisiae)*	NM_001255	90.2	87.9
8	1	*MIHC*	NM_001165	28.8	25.0
	2	Cyclin G1	NM_004060	75.0	64.4
	3	Cell division cycle 20 homolog *(S. cerevisiae)*	NM_001255	90.2	87.9
9	1	Apoptosis inhibitor 1 (baculoviral IAP repeat–containing 3)	NM_001165	28.8	25.0
	2	Cyclin G1	NM_004060	75.0	64.4
	3	Cell division cycle 20 homolog *(S. cerevisiae)*	NM_001255	90.2	87.9
10	1	Nuclear factor (erythroid-derived 2)–like 1	NM_003204	25.0	25.8
	2	Cyclin G1	NM_004060	75.0	63.6
	3	ADP-ribosyltransferase (NAD+; poly [ADP-ribose] polymerase)	NM_001618	88.6	81.8

[a] Genes that present similar expression patterns during IFN and ribavirin combination therapy

ulated among predefined clinical groups than expected by chance, thus enabling the finding of biologically related genes to reinforce one another. GO comparison of gene expression between the patients with CH-C and the healthy volunteers revealed significant differences in the Janus kinase signal transducer and activation of transcription (JAK-STAT) cascade, humoral immune response, and G protein–coupled receptor protein signaling pathway ($P < .005$) (table 3). One-way clustering analyses of representative differentially expressed genes are shown in figure 1*B*. These genes were generally activated in PBMCs from patients with CH-C; however, genes such as *CCR2*, monocyte chemoattractant protein 1 receptor, and *IL7R* were significantly down-regulated. The reason for this is not known, but it may reflect infiltration of PMBCs into the liver. The top 20 differentially expressed genes were selected, and gene-expression profiling of these genes in liver-infiltrating lymphocytes was performed (figure 1*C*). Most of the gene-expression ratios for liver-infiltrating lymphocytes showed >1-fold increases compared with hepatocytes, thus indicating that most genes were preferentially expressed in lymphocytes. Interestingly, the genes with increased expression in liver-infiltrating lymphocytes tended to be expressed at lower levels in PBMCs (figure 1*C*).

Serial changes in the differentially expressed genes listed in table 2 during IFN treatment are shown in figure 2*A*. In the CR group, the expression profiles of genes that were either up-

Table 6. Comparison of ISG expression induced by interferon (IFN).

The table is available in its entirety in the online edition of the *Journal of Infectious Diseases.*